ANTIOXIDANTS & REDOX SIGNALING
Volume 8, Numbers 5 & 6, 2006

Original Research Communication

An Assessment of the Role of Reactive Oxygen Species and Redox Signaling in Norepinephrine-Induced Apoptosis and Hypertrophy of H9c2 Cardiac Myoblasts

MANVEEN K. GUPTA,*[2] T.V. NEELAKANTAN,*[1] MISHRA SANGHAMITRA,[1] RAKESH K. TYAGI,[2] AMIT DINDA,[3] SUBIR MAULIK,[4] CHINMAY K. MUKHOPADHYAY,[2] and SHYAMAL K. GOSWAMI[1,2]

ABSTRACT

Cardiac myocytes, upon exposure to increasing doses of norepinephrine (NE), transit from hypertrophic to apoptotic phenotype. Since reactive oxygen species (ROS) generation is attributed to both phenomena, the authors tested whether an elevation in intracellular ROS level causes such transition. H9c2 cardiac myoblasts upon treatment with hypertrophic and apoptotic doses of NE (2 and 100 μ*M*, respectively) transiently induced intracellular ROS at a comparable level, while 200 μ*M* H_2O_2, another proapoptotic agonist, showed robust and sustained ROS generation. Upon analysis of a number of redox-responsive transcription factors as the downstream targets of ROS signaling, the authors observed that NE (2 and 100 μ*M*) and H_2O_2 (200 μ*M*) were ineffective in inducing NF-κB while both the agonists upregulated AP-1 and Nrf-2. However, the extents of induction of AP-1 and Nrf-2 were not in direct correlation with the respective ROS levels. Also, AP-1 activities induced by two doses of NE were intrinsically different, since at 2 μ*M*, it primarily induced FosB, and at 100 μ*M* it activated Fra-1. Differential induction of FosB and Fra-1 was also reiterated in adult rat myocardium injected with increasing doses of NE. Therefore, NE induces hypertrophy and apoptosis in cardiac myocytes by distinct redox-signaling rather than a general surge of ROS. *Antioxid. Redox Signal.* 8, 1081–1092.

INTRODUCTION

POSTNATAL CARDIAC MYOCYTES are terminally differentiated and are unable to proliferate. Certain pathophysiological conditions leading to cardiac overload elicit an adaptive response by increasing myocyte volume, a condition termed hypertrophy (17, 37). Physiological modulators of cardiac function, such as, endothelin-1, and angiotensin II (Ang II), can mimic hypertrophic response(s) in neonatal and adult myocytes cultured *ex vivo* (40). Signal transducing kinases (e.g., S6, Ras, Raf, ERK, p38), phosphatases (e.g., calcineurin), and downstream transcriptional regulators (e.g., NFAT, GATA-4, NF-κB and MEF-2) have been identified as the mediators of hypertrophic responses (2, 25, 49, 53). It is often observed that some of these agonists (Ang II and NE) also cause apoptosis at higher doses (41, 43). Such transition from hypertrophic to apoptotic "mode" also occurs during end-stage heart failure and is of immense clinical relevance (4, 17, 37). A paradox in the activities of a number of the above-mentioned signaling molecules such as ERK and calcineurin is that these mediate both anti- and proapoptotic responses (6, 36). It remains to be explored how cardiac myocytes utilize apparently similar signaling molecules and still achieve distinctly variable biological consequences.

During recent years, reactive oxygen species (ROS) have drawn considerable attention as a determinant of various biological responses like cell proliferation, tumor progression, hypertrophy, and apoptosis (45). Neonatal rat cardiac my-

[1]School of Life Sciences and [2]Special Centre for Molecular Medicine, Jawaharlal Nehru University; and [3]Department of Pathology and [4]Department of Pharmacology, All India Institute of Medical Sciences, New Delhi, India.
*Both authors have equally contributed to this study.

ocytes, upon exposure to various agonists, induce intracellular ROS followed by hypertrophic response (25, 21). Some of these agonists (e.g., Ang II and NE) at a higher dose also induce ROS followed by apoptosis. Attenuation of ROS by pharmacological and molecular inhibitors mitigates these responses (41, 43). Cardiac myocytes upon treatment with an exogenous oxidant like H_2O_2 at low to moderate doses ($\leq$30 μ*M*) elicit hypertrophic responses, while further increase in concentration (up to 200 μ*M*) leads to apoptosis (33). These studies have thereby evolved a conceptual framework according to which a moderate level of ROS generation leads to hypertrophy and at elevation of a yet unspecified threshold, induces apoptosis (12). In the present study we have examined this concept by studying the effects of norepinephrine (NE) and H_2O_2 on H9c2 cardiac myoblasts. Endogenous ROS levels were measured following respective treatments and its correlation with the induction of a number of redox-responsive transcription factors, further downstream, were studied. We demonstrate that although exposure to NE and H_2O_2 increases intracellular ROS, its level does not necessarily correlate with the downstream events. This indicates the existence of distinctive redox signaling rather than that of a global ROS surge as the determining factor. We finally demonstrate that NE and H_2O_2 initiate cell death by distinctly differing biochemical mechanisms, which is again at variance with the idea of a generalized role of ROS in activating apoptotic programs in cardiac myocytes.

MATERIALS AND METHODS

Materials

All reagents used in this study were from Sigma Aldrich (St. Louis, MO) unless mentioned otherwise. Fetal bovine serum was purchased from Life Technologies (CA), and antibodies were from Cell Signaling (MA), (p65: #3, IκBα: #9242) and Santa Cruz Biotechnologies Inc. (Santa Cruz, CA) (PARP: SC-7150, p50: SC-7178). NF-κB reporter plasmid [$(NF\text{-}\kappa B)_6$-TK-luciferase] and AP-1 reporter plasmid [AP-1-luc (7X)] were from Stratagene (CA), Luciferase assay reagents were purchased from Promega (WI).

Cell culture

H9c2 myoblasts were cultured and maintained as monolayer in Dulbecco's modified Eagle's medium (DMEM), high glucose, supplemented with 10% fetal bovine serum (heat inactivated), 100 units/ml penicillin, 100 μg/ml streptomycin, and 2.5 μg/ml amphotericin B, at 37°C in humidified incubator with 5% CO_2. Subconfluent cells were propagated in 1:6 ratio and were kept in serum-free medium for 24 h prior to treatment with NE (100 m*M* stock in 1 m*M* ascorbic acid) and H_2O_2 (200 m*M* stock).

Primary cardiac myocytes were isolated from neonatal (1–2 days) male Sprague–Dawley rat hearts, according to the method described by Claycomb (11). In brief, excised hearts were finely minced in the ice-cold cell buffer containing 8.10 g/L NaCl, 0.40 g/L KCl, 0.60 g/L $Na_2HPO_4.H_2O$, and 0.90 g/L glucose, and then treated with 0.5 mg/ml collagenase and 0.25 mg/ml hyaluronidase (dissolved in cell buffer) for 15 min at 37°C.

The first batch of dissociated cells were discarded and subsequent batches were pooled and resuspended in DMEM supplemented with 10% heat inactivated fetal bovine serum, 100 units/ml penicillin, 100 μg/ml streptomycin, and 2.5 μg/ml amphotericin B, followed by transferring onto 100 mm dishes. Cells were then kept in a humidified CO_2 incubator at 37°C for 2 h for the attachment of fibroblasts (panning). The supernatant was then transferred to another dish for two more rounds of panning and finally, enriched cardiomyocytes were plated at a density of ~1.5×10^6 cells per 60 mm dishes and grown for 48 h, followed by experimentation. Cells were kept in serum-free medium for 12 h prior to treatment with NE and H_2O_2. At appropriate time points, cells were fixed in methanol and photographed under phase contrast microscope.

MTT assay

Subconfluent cell population was kept overnight in serum-free medium (DMEM) followed by treatment with NE. At appropriate time points, cells were washed in PBS, treated with 50 μl MTT solution (5 mg/ml, tetrazolium salt) and incubated for 2 h at 37°C. Formazan salt crystals were then dissolved in 100 μl of 10 m*M* HCl containing 10% SDS at 37°C overnight. Plates were analyzed in an ELISA plate reader (Labsystems Multiskan RC, Helsinki, Finland) at 570 nm with a reference wavelength of 655 nm.

Measurement of intracellular ROS

The intracellular ROS were measured essentially as described by Chandel *et al*. (9). Cells were kept overnight in serum-free medium and DCFH-DA was added to a final concentration of 5 μ*M*. After 30 min, medium was removed, washed once with PBS, and supplemented with fresh medium. Five min later, agonists under study were added and at different time points cells were washed twice in PBS, lysed in 50 m*M* Tris pH 7.6, 150 m*M* NaCl, 1% NP-40, 0.5% sodium deoxycholate, 0.1% SDS, 1 m*M* phenyl methyl sulfonyl fluoride (PMSF), and 1 μg/ml aprotenin. After centrifugation, lysates were assayed for oxidized H_2DCF in a spectrofluorimeter at 530 nm.

Western blot analysis

Following experimental treatments, H9c2 cells were lysed in 50 m*M* Tris pH 7.6, 400 m*M* NaCl, 1 m*M* EDTA, 1 m*M* EGTA, 1% NP-40, 1 m*M* sodium orthovanadate, 10 m*M* sodium fluoride, 0.5 μg/ml leupeptin, 0.5 μg/ml pepstatin, 0.5 μg/ml aprotinin, and 1 m*M* PMSF. Resolved proteins were then transferred on to Hybond-PVDF membrane (Amersham Pharmacia Biotech, Uppsala, Sweden) followed by Western analysis using respective primary antibodies and HRP conjugated secondary antibody, followed by detection with Western Blotting Chemiluminescence Luminol Reagent (Santa Cruz Biotechnologies, Inc.).

Indirect immunofluorescence studies

Cells grown on sterile glass cover slips were fixed in methanol at −20°C for 15 min, air-dried and then equilibrated in PBS (pH 7.4). Fixed cells were then preincubated thrice with 10 m*M* phosphate buffered saline (PBS) and again

fixed with chilled methanol (−20°C) for 15 min on ice. The cover slips were then washed thrice, air dried and kept at −20°C for 1 h. The cells were then equilibrated in a humidified chamber for 30 min, blocked in 1% bovine serum albumin (BSA) in PBS for 30 min, incubated with primary antibody (1:100 dilution in 1% BSA–PBS), and kept overnight at 4°C. Following washes with PBS, the cells were further incubated for 1 h with Cy-3-conjugated secondary antibody (sheep antirabbit IgG, Sigma; 1:250 dilutions in 1% BSA–PBS) and incubated at room temperature for 1 h. For visualizing cell nuclei, 1 mg/ml DAPI was also included with the secondary antibody. The cells were again washed with PBS and the cover slips were mounted on glass slide and visualized under Axioscope fluorescence microscope (Carl Zeiss, Germany) using suitable filter sets and imaged with the AxioCam camera system coupled to the AxioVision software (Carl Zeiss, Germany).

Transient transfection and reporter assay

Subconfluent population of H9c2 myoblasts grown in 35 mm dishes were transiently transfected with reporter plasmids using Escort IV transfection reagent (Sigma) according to the manufacturer's instructions. Two microgram of plasmid DNA was routinely used per 35 mm dish. Cells were incubated in the transfection reagents in serum-antibiotic-free medium for 8–10 h, refed with fresh serum containing medium, and kept for 12 h. Finally, cells were again kept in serum-free medium for 12 h, followed by the requisite agonist treatments. Cells were then processed for luciferase reporter activity after 4–8 h (~40–48 h posttransfection).

Luciferase reporter assays

Cells were lysed in reporter lysis buffer (Promega). Lysates were then analyzed for the luciferase activities using the Luciferase Reagent Assay Kit (Promega) and readings were taken in a luminometer (Turner Scientific, CA). DNA uptake was normalized by cotransfection of β-galactosidase expression plasmid (pCMV-*gal,* 1 μg). In certain experiments, normalization was also done based on protein content as liposome-mediated plasmid transfer is characterized by uniform transfection efficiency for a set of culture dishes.

Nuclear extract preparation

After respective experimental treatments, cells were lysed in 1 ml of buffer A (20 m*M* HEPES, pH 7.9; 20% glycerol; 10 m*M* NaCl; 1.5 m*M* $MgCl_2$; 0.2 m*M* EDTA; 1 m*M* DTT; 0.1% Triton X-100, protease inhibitors 0.2 m*M* PMSF, 4 μg/ml leupeptin, 10 μg/ml aprotinin, and 2 μg/ml pepstatin). Homogenates were centrifuged at 2,000 rpm at 4°C for 15 min and the nuclear pellets were resuspended in 50 μl of buffer B that was essentially same as buffer A except that it contained 500 m*M* NaCl. The nuclei were lysed in buffer B by incubation on ice with intermittent tapping for 1 h. Lysates were then centrifuged at 10,000 rpm at 4°C for 15 min and the supernatants were aliquoted and snap-frozen at −80°C until used.

Gel mobility shift assay

DNA-protein binding reactions were carried out in 40 μl binding buffer (20 m*M* HEPES, pH 7.9, 5% glycerol, 60 m*M* NaCl, 1.5 m*M* $MgCl_2$, 1.0 m*M* EDTA, and 1.0 m*M* DTT) containing 6–8 μg nuclear extract, 1 μg poly dI-dC, and ^{32}-P-labeled oligonucleotide probe (~40,000 cpm) on ice for 40 min. Protein–DNA complexes were resolved on 8% polyacrylamide gel in 0.5 × TBE for 3 h at 200 V at 4°C.

Immunohistochemistry

Male Sprague–Dawley rats (200–300 g body weight, 2–3 weeks of age) were intraperitoneally injected with three different doses of NE (0.05 mg, 0.2 mg, and 2.5 mg per kg bodyweight) while control rats were injected with normal saline. Hearts were excised 2 and 4 h post treatment and microtransverse sections of the myocardium were mounted on glass slides. Sections were air dried for 2 min, fixed in chilled acetone for 10 min, and stored at −20°C till use. Endogenous peroxidase activity was removed by incubating the sections in methanolic H_2O_2 (0.5%) for 30 min. After rinsing in TBS (pH 7.4), sections were permeabilized by incubating in 0.1% Triton X-100 in TBS and nonspecifically blocked with 1% BSA for 1 h. The sections were then incubated with primary antibody (1:100; in TBST with 0.1% BSA) overnight at 4°C. After washing with TBS, sections were incubated with horseradish peroxidase conjugated secondary antibody (1:200 dilutions in TBST with 0.1% BSA) for 1 h. Peroxidase activity was then visualized with 3′,3′-diaminobenzidine (DAB, 0.04 %) and H_2O_2 (0.015%) in 0.05 *M* TBS. The reaction was stopped in water, sections were air dried, dehydrated in ethanol, cleared in xylene, and mounted in DPX (dibutylphthalate) and photographed in a Nikon microscope. Immunocytochemical controls for the experimental sections were incubated as above with the omission of the primary antibody. Integrity of the myocardium was checked by hematoxylin– eosin staining.

Data analysis

All the experiments were done at least thrice (unless mentioned otherwise) with similar results and representative Figures are shown. Data were collected and expressed as mean ± standard deviation. Significance test (Student *t* test) was performed using Sigma Plot version 8. p values < 0.05, 0.01, and 0.001 are represented as *, **, and ***, respectively.

RESULTS

NE is a moderate and transient inducer of ROS

Neonatal and adult rat cardiac myocytes upon stimulation with NE elicit hypertrophic responses at a lower dose and apoptotic responses at an elevated level (3, 43). The rat cardiac myoblast cell line H9c2 also expresses adrenergic receptors as primary myocytes (13) and has been used for investigating mechanisms of hypertrophy and apoptosis by other agonists (21, 26).

To test the suitability of H9c2 myoblasts for studying hypertrophy and apoptosis induced by NE, we first examined its response to increasing NE concentrations. A subconfluent population of H9c2 cells was treated with increasing doses of NE, and the number of viable cells was measured after 24 h by MTT cell viability assay. Treatment with 2 and 10 μ*M* NE

enhanced the number of viable cells, indicating cell proliferation (Fig. 1A), which was corroborated by photomicrograph (Fig. 1B) and Trypan blue staining (data not shown). Upon further increase in NE concentration (25 μ*M* and above), cells remained quiescent till 24 h (Fig. 1A), beyond which morphological changes characteristic of apoptosis were visible. Forty to sixty hours after NE treatment, ~80% of the cell population underwent apoptosis as confirmed by nuclear condensation (Fig. 1B) and also by the induction of a number of other apoptotic markers as shown below.

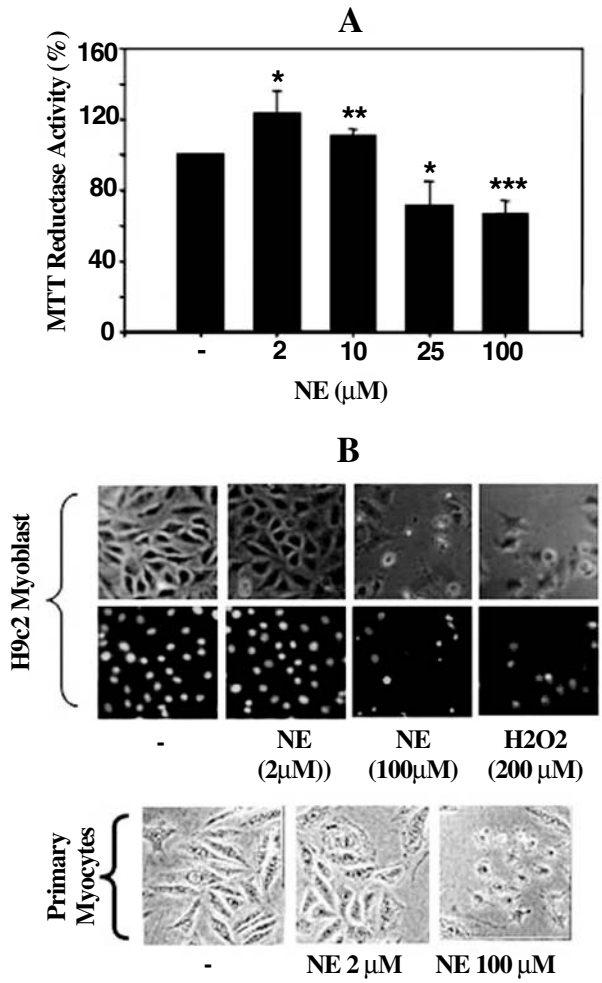

FIG. 1. In H9c2 myoblasts, NE induces cell proliferation at a lower dose and apoptosis at a higher dose. (**A**) H9c2 myoblast cells cultured *in vitro* were treated with increasing doses of NE. Twenty-four hours after treatment, viable cells were assayed by MTT reduction. Values are mean ± SD; $n = 3$; *$p < 0.05$, **$p < 0.01$, and ***$p < 0.001$. (**B,** *top panel*) H9c2 myoblast cells in culture were treated with 2 μ*M* NE, 100 μ*M* NE, and 200 μ*M* H_2O_2. Forty-eight hours after, cells were fixed in chilled methanol and morphology was monitored by phase contrast microscopy. Also nuclear morphology (DAPI stained) was monitored under fluorescent microscope. (**B**, *bottom panel*) Similar analysis was also done with neonatal rat primary cardiac myocytes (For interpretation of the references to color in this figure legend, the reader is referred to the web version of this article).

Thereafter, we measured intracellular ROS levels in NE (2 μ*M* and 100 μ*M*) treated cells with DCFH-DA, a redox-sensitive fluorescent probe. Mammalian cells efficiently take up DCFH-DA and hydrolyze it to its deacetylated form $DCFH_2$, which in turn reacts with intracellular H_2O_2 (and a number of other oxidizing species) generating a highly fluorescent derivative DCF (1, 39). As shown in Fig. 2, both doses of NE generated ROS only transiently (within 15 min) and at a comparable level. For a comparison, we also estimated the level of ROS induced by 200 μ*M* H_2O_2, a concentration that leads to apoptosis to an extent comparable to that by 100 μ*M* NE, albeit at a much faster rate (~8 h, Fig. 1B). Exposure to H_2O_2, however, resulted in more robust and sustained induction of ROS (Fig. 2). Notably, in addition to various reactive oxygen/nitrogen species, a number of other cellular components such as heme, heme proteins, and cytochrome C can also oxidize $DCFH_2$ (1, 8, 39). Nonetheless, oxidation of $DCFH_2$ by heme and heme proteins are relatively slow processes and more cell type specific (39), while that by cytochrome C requires its release from mitochondria to the cytoplasm following onset of apoptosis (8). Therefore, the oxidation of $DCFH_2$ as observed in NE (and H_2O_2) treated cells is likely due to ROS, although its chemical nature is yet to be ascertained.

In cardiac myocytes, upon adrenergic stimulation, alpha-receptor(s) propagate a hypertrophic response; beta-1 receptors propagate an apoptotic response, and beta–2 receptors transmit survival signals (3, 43). Nonetheless, how these signals are integrated at the level of gene expression and eventually lead to a unified response is not understood as yet. In contrast to adrenergic signaling, that by exogenous H_2O_2 is less understood, especially in mammalian cells (48). In the case of cardiac myocytes, it has been proposed that exposure to H_2O_2 leads to the oxidative modifications of membrane constituents that in turn stimulate the Toll-Like Receptor-2 (TLR-2), followed by apoptosis (16). Therefore, intracellular ROS generated by exogenously added H_2O_2 might involve some indirect mechanism such as receptor stimulation, rather than its direct diffusion through the plasma membrane. None-

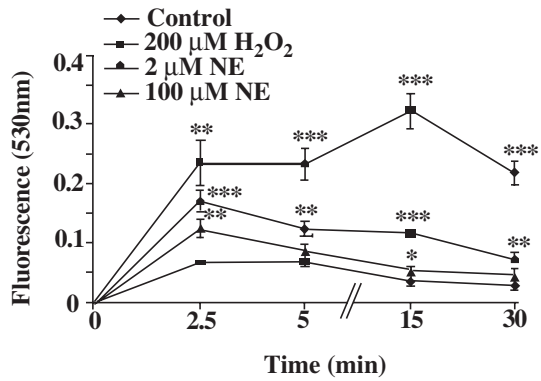

FIG. 2. Differential induction of ROS by NE and H_2O_2. H9c2 cells were treated with 5 μ*M* DCFH-DA for 30 min, followed by treatment with NE (2 μ*M* and 100 μ*M*) and H_2O_2 (200 μ*M*). Cell lysates were then prepared at indicated time points and assayed for oxidized H_2DCF as a measure of intracellular ROS (see Materials and Methods for details). Data shown are mean ± SD; $n = 3$; *$p < 0.05$, **$p < 0.01$, and ***$p < 0.001$.

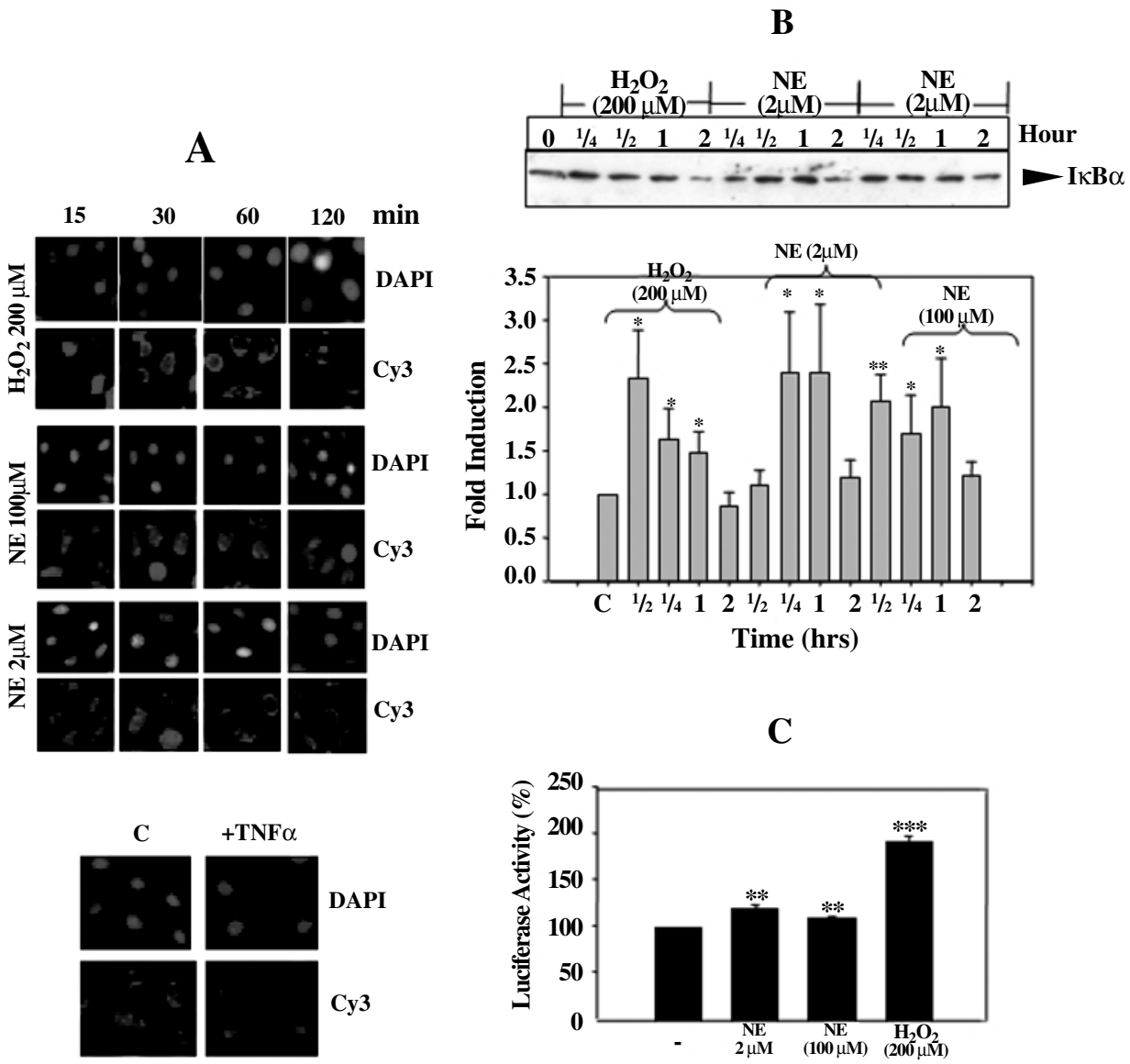

FIG. 3. Both NE and H_2O_2 are weak inducers of NFκB. (**A**) H9c2 cells in culture were treated with NE (2 μ*M* and 100 μ*M*), H_2O_2 (200 μ*M*) and TNF-α (50 ng/ml) followed by indirect immunostaining with anti-p65 and Cy3 conjugated anti-IgG antibody. DAPI staining was done simultaneously to identify the nuclei. Data shown is a representative of four independent experiments with similar results. (**B**) H9c2 cells in culture were treated with NE (2 and 100 μ*M*) and H_2O_2 (200 μ*M*) and total cell extracts were prepared at indicated time points. Forty micrograms of cell extracts were then assayed by immunoblot analysis with IκBα antibody. One representative immunoblot is shown in the *upper panel*. Intensity of respective bands were analyzed densitometrically for three independent experiments and plotted accordingly in the *lower panel*. (**C**) H9c2 cells were transfected with 2.0 μg of NF-κB promoter-luciferase plasmid and ~36 h after transfection, cells were treated with NE and H_2O_2; luciferase activities were assayed after 4 h. For (**B**) and (**C**), values are represented as mean ± SD; $n = 3$; *$p < 0.05$, **$p < 0.01$, and ***$p < 0.001$. (For interpretation of the references to color in this figure legend, the reader is referred to the web version of this article.)

theless, the levels of ROS generated by NE (2 and 100 μ*M*) and H_2O_2 (200 μ*M*) indicate that in cardiac myocytes, even though ROS play a critical role in dictating the downstream events (hypertrophy and apoptosis), its level(s) of induction is not a direct correlate of such consequences.

Increased generation of ROS does not lead to the activation of NF-κB

Transcription factor NF-κB has wide gene regulatory functions including induction of cardiac hypertrophy and survival (10). Numerous studies have shown that diverse signals such as cytokine and growth factor stimulation, UV radiation, and viral infection result in the activation of NF-κB. It has since been proposed that these stimuli lead to the generation of ROS, which in turn activate IκB kinase (IKK) that phosphorylates IκB. Phosphorylated IκB is then degraded, releasing the p65 subunit of NF-κB, followed by its translocation to the nucleus and engagement with the cognate promoters (5). Nevertheless, a nodal role of ROS in NF-κB activation has lately been questioned (23) and other mechanisms of its acti-

vation are emerging (42, 57). We thus examined whether NE (and H_2O_2) treatment leads to the activation of NF-κB and if so, whether the extent(s) of activation is a function of ROS level. As shown in Fig. 3A, nuclear shifts of cytoplasmic p65, a hallmark of NF-κB activation, were assayed by indirect immunofluorescence; both NE and H_2O_2 were only marginally and transiently effective in increasing the nuclear localized p65. Notably, H9c2 myoblasts contain a moderate level of nuclear localized p65 that largely remained unchanged after NE and H_2O_2 treatments. However, treatment with TNF-α resulted in a rapid and robust translocation of p65 to the nucleus (Fig. 3A, lower panel), thereby validating the assay conditions. We thereafter corroborated these observations by immunoblot analysis of IκBα. As shown in Fig. 3B, both NE (2 and 100 μ*M*) and H_2O_2 (200 μ*M*) resulted in an initial increase (~twofold) in IκBα, followed by its partial degradation, albeit with subtle differences in kinetics. In H_2O_2 treated cells, IκBα degradation was incremental reaching ~80% of the preinduction level in 2 h. However, in NE (2 μ*M* at 100 μ*M*) treated cells; maximum degradation occurred only between 1–2 h and still remained slightly above the basal level. Furthermore, both the agonists were equally ineffective in degrading the other subunit of the IκB complex (i.e., IκBβ, data not shown). We thereafter examined the NF-κB specific promoter-reporter assay that showed a modest (~twofold) increase with H_2O_2 treatment and only a marginal (~0.2-fold) increase with NE treatment (Fig. 3C). Taken together, these results demonstrate that although H_2O_2 was more effective than NE in ROS generation, both were poor inducers of NF-κB, thereby indicating the existence of distinct redox-signaling (or otherwise) rather than a general redox-threshold as the modulator of downstream gene regulatory events.

Induction of AP-1 and Nrf-2 is partially related to the ROS level

Besides NF-κB/p65, two other transcription factors (AP-1 and Nrf-2) have also been identified as the mediators of redox-signals to the gene expression machinery. AP-1 is an early responsive heterodimeric (Jun:Fos) transcription factor induced by divergent stimuli including ROS (14, 19, 50). In contrast, Nrf-2 is relatively less studied, especially in the context of its mechanism(s) of activation (38). Nonetheless, recent data indicate that under normal conditions, Nrf-2 is sequestered in the cytoplasm by Keap1 that acts as a redox switch. Upon oxidative stimulation, Keap1 is degraded, thereby releasing Nrf-2, which then translocates to nucleus, binds to antioxidant response elements (ARE) and activates cognate genes (31).

We thus examined the modulation of both Nrf-2 and AP-1 activities as downstream sensors of ROS generation. Nuclear extracts were prepared from NE and H_2O_2 treated cells and assayed for Nrf-2 (ARE: 5′-AATTGCTGACTGACTCAG CATTACT-3′) binding activity. As shown in Fig. 4A, while both NE and H_2O_2 induced Nrf-2, the level of induction was substantially higher in case of 100 μ*M* NE than that for 2 μ*M* NE. On the other hand, both 100 μ*M* NE and 200 μ*M* H_2O_2 induced it at a comparable level. Therefore, although Nrf-2 was induced by both concentrations of NE and by H_2O_2, its extent of induction was not necessarily a function of respective ROS levels. When similar analysis was done with the AP-1 target sequence (TRE: 5′-CGCTTGATGAGTCAGCCGGAA-3'), a moderate induction of AP-1 was observed for 2 μ*M* NE, that was further increased with 100 μ*M* NE (Fig. 4B), and 200 μ*M* H_2O_2 induced it at an even higher level (Fig. 4C). To confirm such pattern of induction of AP-1, we performed AP-1-promoter–reporter analysis (Fig. 4D) and in agreement with the DNA binding assay, higher reporter activity was consistently observed with 100 μ*M* NE (vis-à-vis 2 μ*M* NE). However, similar analysis with H_2O_2-treated cells did not show any detectable increase in luciferase reporter activity (assayed at 2 and 4 h time points). In H9c2 cells and in primary cardiac myocytes, upon treatment with H_2O_2 (apoptotic dose), certain proapoptotic events such as decrease in respiratory complex II and IV activities occur as early as within 20 min, while others such as decrease in membrane potential occurs within 1 h (21, 34). It is thus plausible that following H_2O_2 treatment, although AP-1 and Nrf-2 DNA binding activity increases till 2 h, corresponding reporter gene expression is impaired due to the activation of proapoptotic events. Taken together, these data suggest that in NE- and H_2O_2-treated H9c2 myoblasts, AP-1 and Nrf-2 activities are not modulated by total ROS threshold but by distinctive signaling.

Hypertrophic and apoptotic doses of NE induce two distinct Fos proteins

AP-1 activities consist of heterodimers of Jun (Jun, JunB, and JunD) and Fos (Fos, FosB, Fra-1, and Fra-2) proteins binding to the consensus DNA element $TGA^{G}/_{C}TCA$ (52). Based upon the stimuli and the target cells, multiple AP-1 complexes might be induced in a given condition, but the mechanism(s) by which they recognize their cognate genes is poorly understood (19). In cardiac myocytes (and also in the intact myocardium), agonists such as mechanical stretch, pressure–volume overload, adenosine, angiotensin II, and catecholamines induce AP-1 as an immediate early response (22, 44, 54). We thus argued that, since treatment of cardiac myocytes with low and high doses of NE lead to distinct consequences (hypertrophy and apoptosis), AP-1 activities induced under respective conditions might be intrinsically different (in addition to the difference in their extent of induction, as shown in Fig. 4B).

To test this possibility, we performed immunoblot analysis of various Jun and Fos proteins induced by 2 and 100 μ*M* NE in H9c2 myoblasts. In agreement with the gel mobility shift and reporter assays shown in Fig. 4B and D, both doses of NE induced Jun within 1 h and sustained it till 8 h, the last time point tested (data not shown). On the contrary, both doses of NE initially induced Fos only transiently for 1 h (data not shown) and thereafter, two other members of the Fos family (Fos B and Fra-1) were induced by 2 and 100 μ*M* NE in a reciprocal and dose-dependent manner. As shown in Fig. 5A, μ*M* NE primarily induced Fos B with a peak induction of ~3.6-fold within 2 h, followed by a sustained level (~2.5-fold) until 4 h. On the other hand, 100 μ*M* NE was only a moderate inducer of FosB at the beginning with a peak induction of ~2.2-fold within an hour that was followed by a decline below the basal level. In contrast, Fra-1 was primarily induced by 100 μ*M* NE as a delayed response (~1.7-fold) in 4 h (Fig. 5B). Notably, delayed induction of Fra-1 has also been observed in other cell types, although the relevance is not known yet (7). Also, H9c2 cells had a basal level of Fra-1 that gradually di-

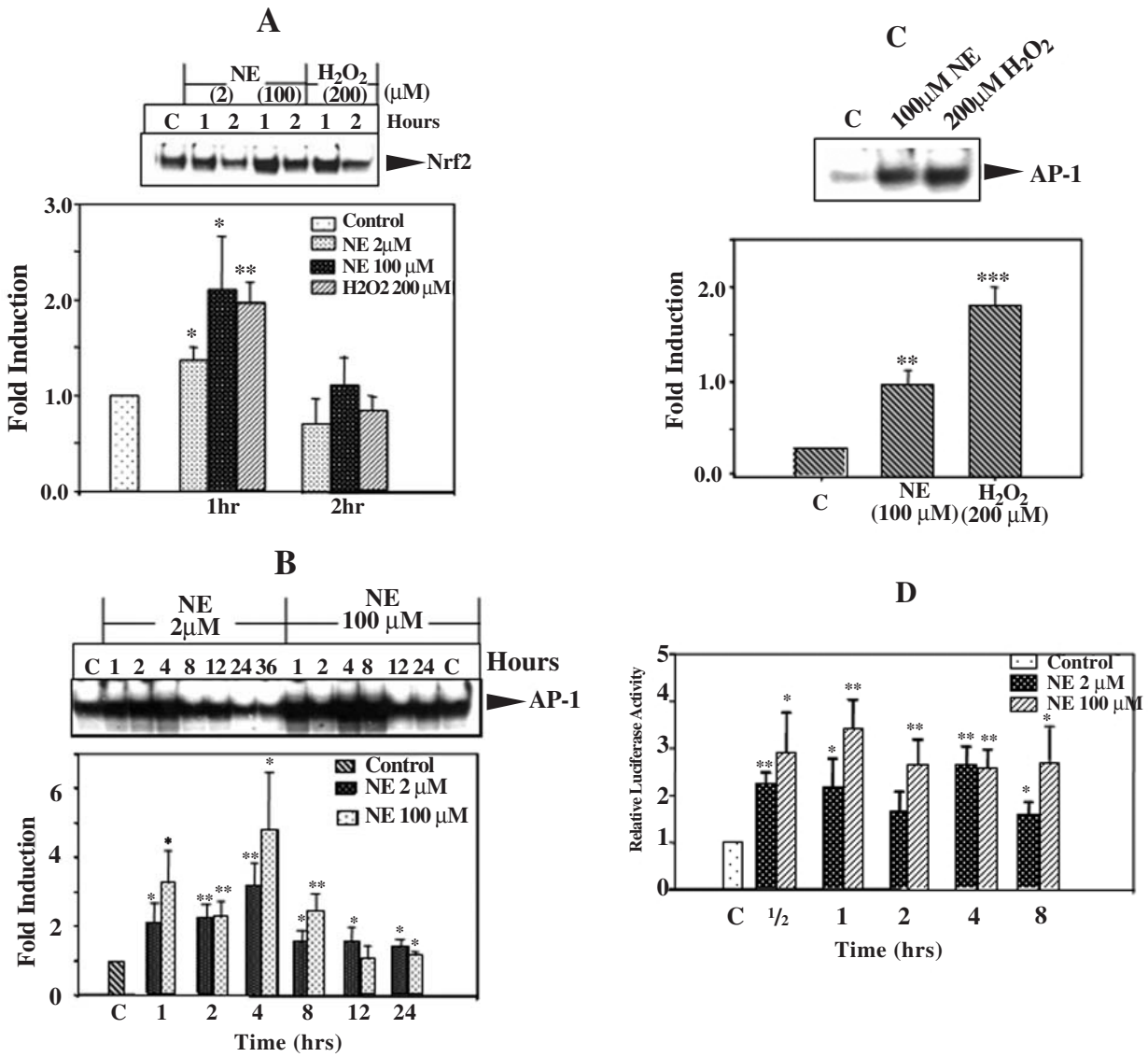

FIG. 4. Induction of AP-1 and Nrf2 activities by NE and H_2O_2. H9c2 cells in culture were treated with NE (2 and 100 μ*M*) and H_2O_2 (200 μ*M*). Nuclear extracts were prepared 1 and 2 h after treatment, and gel mobility shift assays were performed using 8–10 μg nuclear proteins and radiolabeled. (**A**) Nrf-2 (MARE: AATTG CTGACTGACTCAGCATTACT), and (**B** and **C**) AP-1 (TRE: CGCTTGATGAGTCA GCCGGAA) oligonucleotides as probes. DNA binding activity in each lane was estimated densitometrically for three independent experiments and plotted accordingly in the *lower panels*. (**D**) H9c2 cells were transfected with 2.0 μg of AP-1 promoter-luciferase plasmid and ~36 h after transfection, cells were treated with NE. and luciferase activity was assayed at different time points. Values are represented as mean ± SD; $n = 3$; *$p < 0.05$, **$p < 0.01$, and *** $p < 0.001$.

minished after treatment with 2 μ*M* NE (analogous to the decrease in FosB following treatment with 100 μ*M* NE). Since the induction of Fra-1 (by 100 μ*M* NE) was quite moderate, it was further corroborated by transcript analysis and indirect immunostaining of cells treated with increasing doses of NE (data not shown). Noticeably, in the immunoblot, both FosB and Fra-1 appeared as multiple bands, reflective of differential phosphorylation as observed with other cell types (51).

Taken together, it appears that although low and high doses of NE generate comparable levels of ROS, subsequent signaling events are intrinsically different. In view of the significance of such scenario, we thereafter reiterated the differential induction of Fos B and Fra-1 in the *in vivo* context. Adult rats were intraperitoneally injected with three different doses of NE (0.05, 0.2, and 2.5 mg/kg bodyweight) and immunohistochemical analysis of the myocardium were done at 2 and 4 h time points. As shown in Fig. 5C, in agreement with the *ex vivo* analysis done with H9c2 myoblasts (Fig. 5A), increase in Fos B immunoreactivity was seen in the myocardium injected with the lowest dose of NE (0.05 mg/kg bodyweight) and with further increase in NE dose, a lesser degree of induction (0.2 mg/kg body weight, 2 h time point) was followed by diminishment below the background level. Similarly, in agreement with the *ex vivo* analysis, with increasing doses of NE, Fra-1 was increasingly induced and maximum induction was observed with the highest dose (2.5 mg/kg body weight at 4 h;

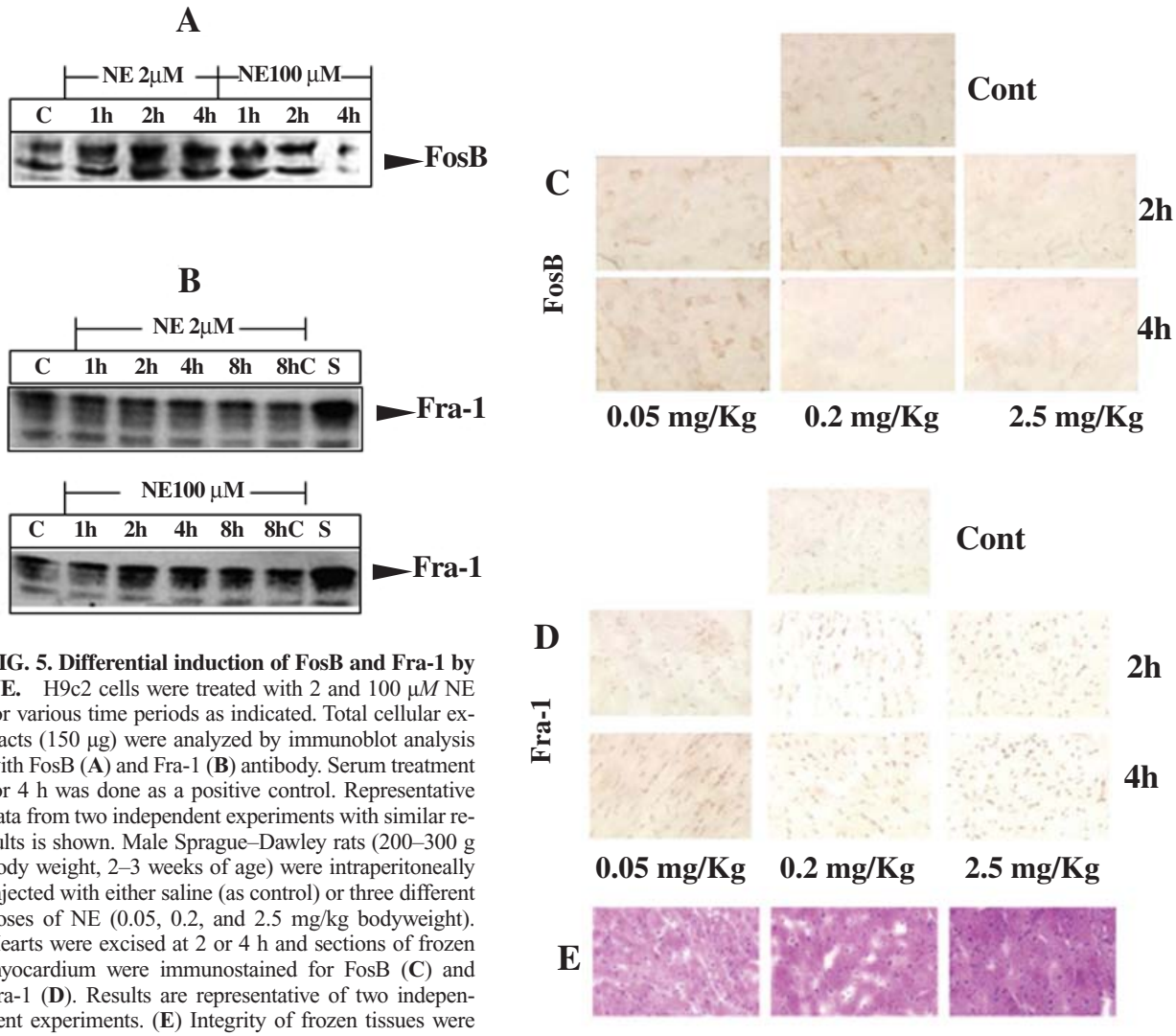

FIG. 5. Differential induction of FosB and Fra-1 by NE. H9c2 cells were treated with 2 and 100 μ*M* NE for various time periods as indicated. Total cellular extracts (150 μg) were analyzed by immunoblot analysis with FosB (**A**) and Fra-1 (**B**) antibody. Serum treatment for 4 h was done as a positive control. Representative data from two independent experiments with similar results is shown. Male Sprague–Dawley rats (200–300 g body weight, 2–3 weeks of age) were intraperitoneally injected with either saline (as control) or three different doses of NE (0.05, 0.2, and 2.5 mg/kg bodyweight). Hearts were excised at 2 or 4 h and sections of frozen myocardium were immunostained for FosB (**C**) and Fra-1 (**D**). Results are representative of two independent experiments. (**E**) Integrity of frozen tissues were checked by hematoxylin–eosin staining and three such randomly picked up sections are shown (**E**).

Fig. 5D). Noticeably, while FosB was induced only in a subpopulation of cells at a moderate level, induction of Fra-1 was more robust, extensive, and distinctively nuclear localized; the reason(s) for which is yet to be explored. Taken together, it appears that the adrenergic signaling observed in H9c2 myoblasts were consistently reproducible in adult rat myocardium injected with various doses of NE.

Norepinephrine and H_2O_2 initiate apoptosis by two distinct mechanisms

Although generation of ROS has been attributed to the induction of apoptosis by both NE and H_2O_2 (12, 43), the precise mechanism by which ROS initiate the death process is not known as yet. Nevertheless, proapoptotic cytokine TNF-α has been identified as the downstream mediator of cell death caused by NE (58), while the mitochondrial death pathway has been attributed to that by H_2O_2 (21, 34). Furthermore, while apoptosis induced by NE is a delayed response (executed after ~48–60 h), that by H_2O_2 is much faster (executed within ~4–8 h). Although our analyses of induction of FosB and Fra-1 by low and high doses NE indicated that distinctive signaling rather than gross ROS level determine the downstream events, we still argued in favor of a common mechanism of initiation apoptosis by NE and H_2O_2. We thus tested the possibility that while a moderate level of ROS generation (by 100 μ*M* NE) causes delayed apoptosis, a surge in ROS results in rapid cell death (programmed) but the triggering mechanisms are the same. To test this concept, we first monitored the kinetic of induction of a number of proapoptotic events: cleavage of PARP, decrease in prosurvival protein Bcl-2, increase in proapoptotic protein Bax, and DNA fragmentation in NE (100 μ*M*) treated cells. As shown in Fig. 6, substantial cleavage of PARP, decrease in Bcl-2 level, increase in Bax, and extensive DNA fragmentation occurred only after 24 h. Notably, in NE-treated cells, morphological manifestation of cell death occurs only after ~36 h and maximum (~80 %) cell death occurs around 48–60 h. Nonetheless, such delayed induction of apoptosis could still be attributed to the immediate early events, as exposure to NE (100 μ*M*) for the initial 3 h was quite adequate in inducing the death program (data not shown).

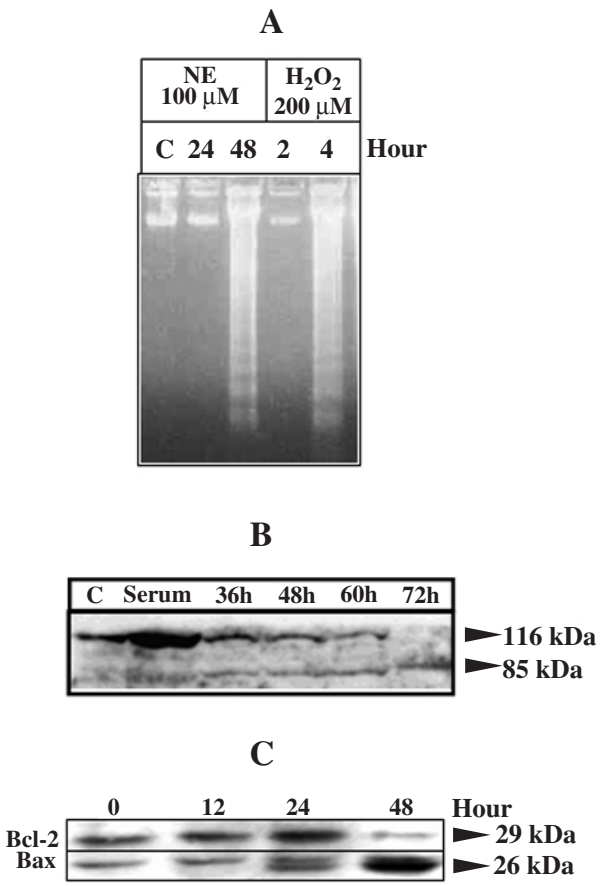

FIG. 6. Kinetic of induction of various markers of apoptosis in NE treated cells. H9c2 cells in culture were treated with 100 μ*M* NE. (**A**) Total cellular DNA isolated at time points as indicated above were resolved on 1.2% agarose gel. Also for a comparison, DNA isolated from H_2O_2 (200 μ*M*) treated cells (8 h) was analyzed simultaneously. (**B**) Sixty microgram of total cellular proteins was subjected to immunoblot analysis with anti-PARP antibody. The uncleaved and cleaved PARP proteins are identified by their respective molecular weights (116 and 85 kD). (**C**) Seventy microgram total cellular proteins were analyzed for Bcl-2 and Bax proteins using respective antibodies.

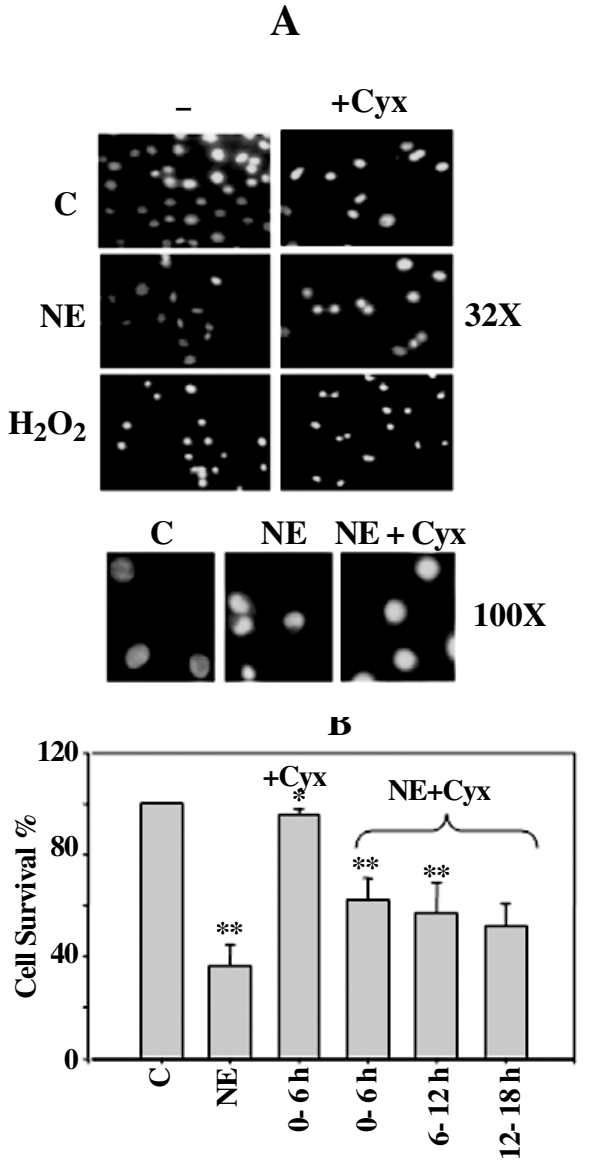

FIG. 7. Apoptosis induced by NE requires *de novo* protein synthesis but that by H_2O_2 does not. (**A**) H9c2 cells were treated with 100 μ*M* NE and 200 μ*M* H_2O_2 in presence or in absence of cycloheximide (10 μg/ml). Eight hours after H_2O_2 treatment and 48 h after NE treatment, cell nuclei were stained with DAPI and observed under fluorescence microscope for the presence of condensed nuclei. (**B**) Following NE treatment, prevention of cell death by cycloheximide, when added at different time points, was also assayed by MTT reduction. Values are represented as mean ± SD; $n = 3$; $^*p < 0.05$, $^{**}p < 0.01$, and $^{***}p < 0.001$. (For interpretation of the references to color in this figure legend, the reader is referred to the web version of this article.)

Therefore, cell death induced by NE might be an indirect consequence of ROS generation that occurs only transiently and moderately (and also at the same level as that induced by 2 μ*M* NE) immediately after NE treatment.

This prompted us to believe that while the induction of apoptosis by NE is a secondary event following ROS generation, that in the case of H_2O_2 is the direct result of surge in ROS, and therefore, the two processes are intrinsically different. We thus treated cells with cycloheximide (10 μg/ml), a reversible inhibitor of protein synthesis, along with NE and H_2O_2, and monitored the extent of cell death. As shown in Fig. 7, while cycloheximide substantially prevented cell death by NE, it was ineffective for H_2O_2. Furthermore, the protective effect of cycloheximide was highest only when the treatment was done for the first 6 h of NE treatment. Such results, therefore, unambiguously established that while onset of apoptosis by NE requires *de novo* protein synthesis at the beginning, that by H_2O_2 does not have such a requirement. Thus, the biochemical mechanism by which H9c2 myoblasts sense and process the apoptotic (and hypertrophic) signal(s) are qualitatively different for NE and H_2O_2 and therefore, plausibly involve distinct redox-signaling rather than a general surge of ROS as the determining factor.

DISCUSSION

The present study was undertaken to examine the tenet that intracellular ROS level plays a nodal role in determining events like hypertrophy and apoptosis in cardiac myocytes. Cardiac hypertrophy is characterized by multiple criteria, manifestation of which may vary from one agonist to another, thereby indicating integration of multiple signal inputs (4, 17). The existence of multiple pathways for the induction of cell death in cardiac myocytes has also been observed but the precise mechanism(s) remains to be investigated (20, 32, 46). Over the years, ROS has been perceived as a biological hazard causing oxidative damage to the cellular components leading to cancer, neuro-, and cardiovascular degeneration, and disorders related to aging (35). More recent studies reveal that ROS also have roles in modulating normal cellular functions such as cell proliferation, angiogenesis, and DNA replication (15). Furthermore, although oxidative stress is often used as a synonym for ROS generation, general oxidative stress is different from redox signaling although the parameters are yet to be clearly defined (15, 18). In this context, comparative analysis of the intensity of ROS generation by 2 μ*M* NE, 100 μ*M* NE, and 200 μ*M* H_2O_2 subscribe to the existence of distinct signaling mechanisms rather than a general ROS threshold as the factor deciding whether to activate the hypertrophic or apoptotic pathways.

To have an insight into the downstream events following ROS generation, we have examined the induction of NF-κB, a well-investigated redox-sensitive transcription factor. Although it has long been considered that various agonists activate NF-κB by a common mediator like ROS, certain discrepancies *viz.,* the temporal differences between the ROS generation and the activation of NF-κB has often been cited as evidence against a nodal role of ROS (5). Such arguments have further been strengthened by some recent observations like (i) activation of NF-κB can be functionally dissociated from the generation of ROS by NADPH oxidase and (ii) antioxidant *N*-acetyl cysteine inhibits the induction of NF-κB by a mechanism independent of attenuating ROS (23). Our observation that the translocation of p65 from cytoplasm to the nucleus is not a correlate to ROS threshold also agrees with similar studies in other cell types and thereby indicates interplay between multiple signaling components rather than a single factor like ROS generation (29). Furthermore, marginal and slow translocation of p65 following NE and H_2O_2 treatment vis-à-vis a rapid and substantial translocation by TNF-α is also in agreement with studies done with primary myocytes (16) and therefore is not an aberration due to the use of H9c2 myoblast as the test system. In contrast to poor induction of NF-κB, the extent of induction of both AP-1 and Nrf-2 by NE and H_2O_2 were substantial, though not necessarily a function of the ROS level. Taken together, it appears that induction of hypertrophy and apoptosis by NE involves integration of multiple inputs to which ROS might be contributing in a context specific manner.

In metazoan cells, cross talk between various signaling cascades is a highly evolved mechanism of signal augmentation (24), signal attenuation (56), and signal sustenance (30). In this context, our observation that although both doses of NE induce Jun and Fos, they act differentially while inducing FosB and Fra-1 is significant, as it exemplifies how signals emanating from multiple adrenergic receptors are differentially integrated further downstream. The significance of this differential adrenergic signaling leading to the induction two distinct forms of AP-1 (comprising FosB and Fra-1), respectively, by 2 and 100 μ*M* NE was further strengthened by its reproduction *in vivo*. Furthermore, while in the case of FosB the responses were limited to a subpopulation of cells in the myocardium, induction of Fra-1 was observed in a much wider population, the significance of which is yet to be understood. Nonetheless, it has often been observed that under a given pathological condition, only a subpopulation of myocytes undergo apoptosis (and/or hypertrophy). Although both FosB and Fra-1 have generally been implicated in cell proliferation and differentiation, recent studies have also implicated Fra-1 in a number of other contexts such as tumorigenesis and increased apoptosis (47), experimentally induced heart failure (55), and cardiomyocyte apoptosis associated with cardiomyopathy (44).

Cell signaling machinery in higher eukaryotes integrates extracellular stimuli with the genetic apparatus with remarkable speed and specificity. Thousands of G protein couple receptors use a fairly small pool of second messengers and still remain functionally distinct. Recent studies suggest that such signal specificity is mediated by multiprotein signaling complexes formed in the raft microdomains (27, 28). Taken together, this study does not undermine the role of ROS as the determining factor for either hypertrophy or apoptosis. Rather, it is likely that hypertrophic and apoptotic signals generated by NE (and H_2O_2) are propagated by distinct redox mediators rather than by the generation of a cell wide pool of ROS. Thus, further understanding of the mechanisms of hypertrophy and apoptosis in cardiac myocytes will require a composite knowledge of the source, chemical nature, and the downstream targets of the ROS that is generated only transiently at the very beginning of the signaling process. Current work is in progress to that direction.

ACKNOWLEDGMENTS

Manveen K. Gupta and T.V. Neelakantan were the recipients of Junior Research fellowships from the Council of Scientific and Industrial Research, India. The research work was supported by the grants awarded to S.K. Goswami by the Department of Biotechnology, Govt of India and the University Grants Commission, India (under the University with Potential for Excellence Programme). We acknowledge Prof. D.P. Sarkar, Department of Biochemistry, Delhi University South Campus, New Delhi, for generous material help. We also acknowledge Sanghamitra Mishra and Amrita Mishra for linguistic improvement of the manuscript.

ABBREVIATIONS

Ang II, angiotensin II; DAPI, 4,6-diamidino-2-phenylindole; DCFHDA, 2', 7'-dichlorofluorescin diacetate; DCF, dichlorofluorescin; DMEM, Dulbecco's modified Eagle's medium; DTT, dithiothreitol; ERK, extracellular signal-responsive kinase; MEF-2, myocyte enhancer factor-2; MTT, methylthiazoletetrazolium; NE, norepinephrine; NFAT, nu-

clear factor of activated T-cells; Nrf-2, nuclear respiratory factor-2; PARP, poly (ADP-ribose) polymerase; PBS, phosphate buffered saline; PMSF, phenyl methyl sulfonyl fluoride; ROS, reactive oxygen species; TBE, Tris, borate, EDTA buffer; TBS, Tris buffered saline; TLR-2, toll-like receptor-2; TNF-α, tumor necrosis factor–α; TRE, TPA response element.

REFERENCES

1. Afzal M, Matsugo S, Sasai M, Xu B, Aoyama K, and Takeuchia T. Method to overcome photoreaction, a serious drawback to the use of dichlorofluorescin in evaluation of reactive oxygen species. *Biochem Biophys Res Commun* 304: 619–624, 2003.
2. Akazawa H and Komuro I. Roles of cardiac transcription factors in cardiac hypertrophy. *Circ Res* 92: 1079–1088, 2003.
3. Barki-Harrington L, Perrino C, and Rockman HA. Network integration of the adrenergic system in cardiac hypertrophy. *Cardiovasc Res* 63: 391–402, 2004.
4. Booz GW, Day JN, and Baker KM. Interplay between the cardiac renin angiotensin system and JAK-STAT signaling: role in cardiac hypertrophy, ischemia/reperfusion dysfunction, and heart failure. *J Mol Cell Cardiol* 34: 1443–1453, 2002.
5. Bowie A and O'Neill LA. Oxidative stress and nuclear factor-κB activation: a reassessment of the evidence in the light of recent discoveries. *Biochem Pharmacol* 59: 113–123, 2000.
6. Bueno OF and Molkentin JD. Involvement of extracellular signal-regulated kinases 1/2 in cardiac hypertrophy and cell death. *Circ Res* 91: 776 –781, 2002.
7. Burch PM, Yuan Z, Loonen A, and Heintz NH. An extracellular signal-regulated kinase 1- and 2-dependent program of chromatin trafficking of c-Fos and Fra-1 is required for cyclin D1 expression during cell cycle reentry. *Mol Cell Biol* 24: 4696–4709, 2004.
8. Burkitt MJ and Wardman P. Cytochrome C is a potent catalyst of dichlorofluorescin oxidation: Implications for the role of reactive oxygen species in apoptosis. *Biochem Biophys Res Commun* 282: 329–333, 2001.
9. Chandel NS, Schumacker PT, and Arch RH. Reactive oxygen species are downstream products of TRAF-mediated signal transduction. *J Biol Chem* 276: 42728–42736, 2001.
10. Chen LF and Greene WC. Shaping the nuclear action of NF-κB. *Nat Rev Mol Cell Biol* 5: 392–401, 2004.
11. Claycomb WC. Culture of cardiac muscle cells in serum-free media. *Exp Cell Res* 131: 231–236, 1981.
12. Clerk A. The radical balance between life and death. *J Mol Cell Cardiol* 35: 599–602, 2003.
13. Dangel V, Giray J, Ratge D, and Wisser H. Regulation of beta-adrenoceptor density and mRNA levels in the rat heart cell-line H9c2. *Biochem J* 317: 925–931, 1996.
14. Eferl R and Wagner EF. AP-1: a double-edged sword in tumorigenesis. *Nat Rev Cancer* 3: 859–868, 2003.
15. Forman HJ, Fukuto JM, and Torres M. Redox signaling: thiol chemistry defines which reactive oxygen and nitrogen species can act as second messengers. *Am J Physiol Cell Physiol* 287: C246–256, 2004.
16. Frantz S, Kelly RA, and Bourcier T. Role of TLR-2 in the activation of nuclear factor kappaB by oxidative stress in cardiac myocytes. *J Biol Chem* 276: 5197–5203, 2001.
17. Frey N and Olson EN. Cardiac hypertrophy: the good, the bad, and the ugly. *Annu Rev Physiol* 65: 45–79, 2003.
18. Gerald D, Berra E, Frapart YM, Chan DA, Giaccia AJ, Mansuy D, Pouyssegur J, Yaniv M, and Mechta–Grigoriou F. JunD reduces tumor angiogenesis by protecting cells from oxidative stress. *Cell* 118: 781–794, 2004.
19. Hess J, Angel P, and Schorpp–Kistner M. AP-1 subunits: quarrel and harmony among siblings. *J Cell Sci* 117: 5965–5973, 2004.
20. Graham RM, Frazier DP, Thompson JW, Haliko S, Li H, Wasserlauf BJ, Spiga MG, Bishopric NH, and Webster KA. A unique pathway of cardiac myocyte death caused by hypoxia-acidosis. *J Exp Biol* 207: 3189–3200, 2004.
21. Han H, Long H, Wang H, Wang J, Zhang Y, and Wang Z. Progressive apoptotic cell death triggered by transient oxidative insult in H9c2 rat ventricular cells: a novel pattern of apoptosis and the mechanisms. *Am J Physiol Heart Circ Physiol* 286: H2169–2182, 2004.
22. Hannan RD, Stennard FA, and West A. Expression of c-fos and related genes in the rat heart in response to norepinephrine. *J Mol Cell Cardiol* 25: 1137–1148, 1993.
23. Hayakawa M, Miyashita H, Sakamoto I, Kitagawa M, Tanaka H, Yasuda H, Karin M, and Kikugawa K. Evidence that reactive oxygen species do not mediate NF-kappaB activation. *EMBO J* 22: 3356–3366, 2003.
24. Hendriks BS, Orr G, Wells A, Wiley HS, and Lauffenburger DA. Parsing ERK activation reveals quantitatively equivalent contributions from epidermal growth factor receptor and HER2 in human mammary epithelial cells. *J Biol Chem* 280: 6157–6169, 2005.
25. Hirotani S, Otsu K, Nishida K, Higuchi Y, Morita T, Nakayama H, Yamaguchi O, Mano T, Matsumura Y, Ueno H, Tada M, and Hori M. Involvement of nuclear factor-κB and apoptosis signal-regulating kinase 1 in G-protein-coupled receptor agonist-induced cardiomyocyte hypertrophy. *Circulation* 105: 509–515, 2002.
26. Huang CY, Kuo WW, Chueh PJ, Tseng CT, Chou MY, and Yang JJ. Transforming growth factor-beta induces the expression of ANF and hypertrophic growth in cultured cardiomyoblast cells through ZAK. *Biochem Biophys Res Commun* 324: 424–431, 2004.
27. Hueber AO. Role of membrane microdomain rafts in TNFR-mediated signal transduction. *Cell Death Differ* 10: 7–9, 2003.
28. Hur EM and Kim KT. G protein-coupled receptor signaling and cross-talk: achieving rapidity and specificity. *Cell Signal* 14: 397–405, 2002.
29. Ito K, Hanazawa T, Tomita K, Barnes PJ, and Adcock IM. Oxidative stress reduces histone deacetylase 2 activity and enhances IL-8 gene expression: role of tyrosine nitration. *Biochem Biophys Res Commun* 315: 240–245, 2004.
30. Kamata H, Honda S, Maeda S, Chang L, Hirata H, and Karin M. Reactive oxygen species promote TNFα-induced death and sustained JNK activation by inhibiting MAP kinase phosphatases. *Cell* 120: 649–661, 2005.
31. Kobayashi A, Ohta T, and Yamamoto M. Unique function of the Nrf2-Keap1 pathway in the inducible expression of

antioxidant and detoxifying enzymes. *Methods Enzymol* 378: 273–286, 2004.
32. Kostin S, Pool L, Elsasser A, Hein S, Drexler HC, Arnon E, Hayakawa Y, Zimmermann R, Bauer E, Klovekorn WP, and Schaper J. Myocytes die by multiple mechanisms in failing human hearts. *Circ Res* 92: 715–724, 2003.
33. Kwon SH, Pimentel DR, Remondino A, Sawyer DB, and Colucci WS. H_2O_2 regulates cardiac myocyte phenotype via concentration-dependent activation of distinct kinase pathways. *J Mol Cell Cardiol* 35: 615–621, 2003.
34. Long X, Goldenthal MJ, Wu G, and Marín-García J. Mitochondrial Ca^{2+} flux and respiratory enzyme activity decline are early events in cardiomyocyte response to H_2O_2. *J Mol Cell Cardiol* 37: 63–70, 2004.
35. Molavi B and Mehta JL. Oxidative stress in cardiovascular disease: molecular basis of its deleterious effects, its detection, and therapeutic considerations. *Curr Opin Cardiol* 19: 488–493, 2004.
36. Molkentin JD. Calcineurin, mitochondrial membrane potential, and cardiomyocyte apoptosis. *Circ Res* 88: 1220–1222, 2001.
37. Nadal-Ginard B, Kajstura J, Leri A, and Anversa P. Myocyte death, growth, and regeneration in cardiac hypertrophy and failure. *Circ Res* 92: 139–150, 2003.
38. Nguyen T, Yang CS, and Pickett CB. The pathways and molecular mechanisms regulating Nrf2 activation in response to chemical stress. *Free Radic Biol Med* 37: 433–441, 2004.
39. Ohashi T, Mizutani A, Murakami A, Kojo S, Ishii T, and Taketani S. Rapid oxidation of dichlorodihydrofluorescin with heme and hemoproteins: formation of the fluorescein is independent of the generation of reactive oxygen species. *FEBS Lett* 511: 21–27, 2002.
40. Olson EN. A decade of discoveries in cardiac biology. *Nat Med* 10: 467–474, 2004.
41. Pang JJ, Xu RK, Xu XB, Cao JM, Ni C, Zhu WL, Asotra K, Chen MC, and Chen C. Hexarelin protects rat cardiomyocytes from angiotensin II-induced apoptosis *in vitro*. *Am J Physiol Heart Circ Physiol* 286: H1063–1069, 2004.
42. Rahman I, Marwick J, and Kirkham P. Redox modulation of chromatin remodeling: impact on histone acetylation and deacetylation, NF-κB and proinflammatory gene expression. *Biochem Pharmacol* 68: 1255–1267, 2000.
43. Remondino A, Kwon SH, Communal C, Pimentel DR, Sawyer DB, Singh K, and Colucci WS. Beta-adrenergic receptor-stimulated apoptosis in cardiac myocytes is mediated by reactive oxygen species/c-Jun NH2-terminal kinase-dependent activation of the mitochondrial pathway. *Circ Res* 92: 136–138, 2003.
44. Ricci R., Eriksson U., Oudit GY., Eferl R, Akhmedov A, Sumara I, Sumara G, Kassiri Z, David JP, Bakiri L, Sasse B, Idarraga MH, Rath M, Kurz D, Theussl HC, Perriard JC, Backx P, Penninger JM, and Wagner EF. Distinct functions of junD in cardiac hypertrophy and heart failure. *Genes Dev* 19: 208–213, 2005.
45. Sabri A, Hughie HH, and Lucchesi PA. Regulation of hypertrophic and apoptotic signaling pathways by reactive oxygen species in cardiac myocytes. *Antioxid Redox Signal* 5: 731–740, 2003.
46. Sharov VG, Todor A, Suzuki G, Morita H, Tanhehco EJ, and Sabbah HN. Hypoxia, angiotensin-II, and norepinephrine mediated apoptosis is stimulus specific in canine failed cardiomyocytes: a role for p38 MAPK, Fas-L and cyclin D1. *Eur J Heart Fail* 5: 121–129, 2003.
47. Shirsat NV and Shaikh SA. Overexpression of the immediate early gene fra-1 inhibits proliferation, induces apoptosis, and reduces tumourigenicity of c6 glioma cells. *Exp Cell Res* 291: 91–100, 2003.
48. Stone JR. An assessment of proposed mechanisms for sensing hydrogen peroxide in mammalian systems. *Arch Biochem Biophys* 422: 119–124, 2004.
49. Sugden PH. Signaling pathways in cardiac myocyte hypertrophy. *Ann Med* 33: 611–622, 2001.
50. Tell G, Damante G, Caldwell D, and Kelley MR. The intracellular localization of APE1/Ref-1: more than a passive phenomenon. *Antioxid Redox Signal* 7: 367–384, 2005.
51. Vial E and Marshall CJ. Elevated ERK-MAP kinase activity protects the FOS family member FRA-1 against proteasomal degradation in colon carcinoma cells. *J Cell Sci* 11: 4957–4963, 2003.
52. Vinson C, Myakishev M, Acharya A, Mir AA, Moll JR, and Bonovich M. Classification of human B-ZIP proteins based on dimerization properties. *Mol Cell Biol* 22: 6321–6335,. 2002.
53. Wang W, Zhu W, Wang S, Yang D, Crow MT, Xiao RP, and Cheng H. Sustained beta1-adrenergic stimulation modulates cardiac contractility by Ca^{2+}/calmodulin kinase signaling pathway. *Circ Res* 95: 798–806, 2004.
54. Webster KA, Discher DJ, and Bishopric NH. Induction and nuclear accumulation of fos and jun protooncogenes in hypoxic cardiac myocytes. *J Biol Chem* 268: 16852–16858, 1993.
55. Wellner M, Dechend R, Park JK, Shagdarsuren E, Al Saadi N, Kirsch T, Gratze P, Schneider W, Meiners S, Fiebeler A, Haller H, Luft FC, and Muller DN. Cardiac gene expression profile in rats with terminal heart failure and cachexia. *Physiol Genomics* 20: 256–267, 2005.
56. Williamson DL, Kimball SR, and Jefferson LS. Acute treatment with TNF-α attenuates insulin-stimulated protein synthesis in cultures of C2C12 myotubes through a MEK1-sensitive mechanism. *Am J Physiol Endocrinol Metab* 289: E95–104, 2005.
57. Wu S, Tan M, Hu Y, Wang JL, Scheuner D, and Kaufman RJ. Ultraviolet light activates NF-κB through translational inhibition of IκBα synthesis. *J Biol Chem* 279: 34898–34902, 2004.
58. Yun-Ching F, Ching-Shiang C, Sui-Chu Y, Betau H, Yung-Tsung C, and Shih-Lan H. Norepinephrine induces apoptosis in neonatal rat cardiomyocytes through a reactive oxygen species–TNFα–caspase signaling pathway. *Cardiovasc Res* 62: 558–567, 2004.

Address reprint requests to:
Dr. Shyamal K. Koswami
School of Life Sciences
Jawaharlal Nehru University
New Delhi 110067, India

E-mail: skgoswami@mail.jnu.ac.in

Date of first submission to ARS Central, September 23, 2005; date of acceptance, December 1, 2005.

This article has been cited by:

1. Md. Mushtaque, Fernando Avecilla, Amir Azam. 2012. Synthesis, characterization and structure optimization of a series of thiazolidinone derivatives as Entamoeba histolytica inhibitors. *European Journal of Medicinal Chemistry* **55**, 439-448. [CrossRef]
2. Subir Kumar Maulik, Santosh Kumar. 2012. Oxidative stress and cardiac hypertrophy: a review. *Toxicology Mechanisms and Methods* 1-8. [CrossRef]
3. Mohmmad Younus Wani, Abdul Roouf Bhat, Amir Azam, Inho Choi, Fareeda Athar. 2012. Probing the antiamoebic and cytotoxicity potency of novel tetrazole and triazine derivatives. *European Journal of Medicinal Chemistry* **48**, 313-320. [CrossRef]
4. Sheikh Shreaz, Rimple Bhatia, Neelofar Khan, Sheikh Imran Ahmad, Sumathi Muralidhar, Seemi F. Basir, Nikhat Manzoor, Luqman A. Khan. 2011. Interesting anticandidal effects of anisic aldehydes on growth and proton-pumping-ATPase-targeted activity. *Microbial Pathogenesis* **51**:4, 277-284. [CrossRef]
5. Zhiyou Cai, Bin Zhao, Anna Ratka. 2011. Oxidative Stress and #-Amyloid Protein in Alzheimer's Disease. *NeuroMolecular Medicine* . [CrossRef]
6. Rayees Ahmad Sheikh, Mohmmad Younus Wani, Sheikh Shreaz, Athar Adil Hashmi. 2011. Synthesis, characterization and biological screening of some Schiff base macrocyclic ligand based transition metal complexes as antifungal agents. *Arabian Journal of Chemistry* . [CrossRef]
7. Abdul R. Bhat, Tazeem, Amir Azam, Inho Choi, Fareeda Athar. 2011. 3-(1,3,4-Thiadiazole-2-yl)quinoline derivatives: Synthesis, characterization and anti-microbial activity. *European Journal of Medicinal Chemistry* **46**:7, 3158-3166. [CrossRef]
8. Ekta Jindal, Shyamal K. Goswami. 2011. In cardiac myoblasts, cellular redox regulates FosB and Fra-1 through multiple cis-regulatory modules. *Free Radical Biology and Medicine* . [CrossRef]
9. Mohmmad Younus Wani, Fareeda Athar, Attar Salauddin, Subhash Mohan Agarwal, Amir Azam, Inho Choi, Abdul Roouf Bhat. 2011. Novel terpene based 1,4,2-dioxazoles: Synthesis, characterization, molecular properties and screening against Entamoeba histolytica. *European Journal of Medicinal Chemistry* . [CrossRef]
10. Sheikh Shreaz, Rimple Bhatia, Neelofar Khan, Sumathi Muralidhar, Seemi F. Basir, Nikhat Manzoor, Luqman Ahmad Khan. 2011. Spice oil cinnamaldehyde exhibits potent anticandidal activity against fluconazole resistant clinical isolates. *Fitoterapia* . [CrossRef]
11. Sheikh Shreaz, Rayees A. Sheikh, Rimple Bhatia, Khan Neelofar, Sheikh Imran, Athar A. Hashmi, Nikhat Manzoor, Seemi F. Basir, Luqman A. Khan. 2011. Antifungal activity of #-methyl trans cinnamaldehyde, its ligand and metal complexes: promising growth and ergosterol inhibitors. *BioMetals* . [CrossRef]
12. Silvia Cetrullo, Benedetta Tantini, Annalisa Facchini, Carla Pignatti, Claudio Stefanelli, Claudio Marcello Caldarera, Flavio Flamigni. 2011. A pro-survival effect of polyamine depletion on norepinephrine-mediated apoptosis in cardiac cells: role of signaling enzymes. *Amino Acids* **40**:4, 1127-1137. [CrossRef]
13. Sheikh Shreaz, Rimple Bhatia, Neelofar Khan, Sumathi Muralidhar, Seemi F. Basir, Nikhat Manzoor, Luqman Ahmad Khan. 2011. Exposure of Candida to p-anisaldehyde inhibits its growth and ergosterol biosynthesis. *The Journal of General and Applied Microbiology* **57**:3, 129-136. [CrossRef]
14. Yamuna Devi Paila, Ekta Jindal, Shyamal K. Goswami, Amitabha Chattopadhyay. 2011. Cholesterol depletion enhances adrenergic signaling in cardiac myocytes. *Biochimica et Biophysica Acta (BBA) - Biomembranes* **1808**:1, 461-465. [CrossRef]
15. Amardeep Jaiswal, Santosh Kumar, Sandeep Seth, Amit Kumar Dinda, Subir Kumar Maulik. 2010. Effect of U50,488H, a #-opioid receptor agonist on myocardial #-and #-myosin heavy chain expression and oxidative stress associated with isoproterenol-induced cardiac hypertrophy in rat. *Molecular and Cellular Biochemistry* **345**:1-2, 231-240. [CrossRef]
16. Fabio Galetta, Ferdinando Franzoni, Giampaolo Bernini, Fallawi Poupak, Angelo Carpi, Giuseppe Cini, Leonardo Tocchini, Alessandro Antonelli, Gino Santoro. 2010. Cardiovascular complications in patients with pheochromocytoma: A mini-review. *Biomedicine & Pharmacotherapy* **64**:7, 505-509. [CrossRef]
17. Chong-Feng Bai, Jin-Cheng Liu, Rong Zhao, Wei Cao, Shui-Bin Liu, Xiao-Nan Zhang, Hong-Ju Guo, Qi Yang, Ding-Hua Yi, Ming-Gao Zhao. 2010. Role of 5-HT2B receptors in cardiomyocyte apoptosis in noradrenaline-induced cardiomyopathy in rats. *Clinical and Experimental Pharmacology and Physiology* **37**:7, e145-e151. [CrossRef]

18. Michael YC Tsang, Simon W Rabkin. 2009. p38 MITOGEN-ACTIVATED PROTEIN KINASE (MAPK) IS ACTIVATED BY NORADRENALINE AND SERVES A CARDIOPROTECTIVE ROLE, WHEREAS ADRENALINE INDUCES p38 MAPK DEPHOSPHORYLATION. *Clinical and Experimental Pharmacology and Physiology* **36**:8, e12-e19. [CrossRef]
19. Xiang-Chun Shen, Zhi-Yu Qian, Ya-Juan Wang, Jin-Ao Duan. 2009. Crocetin attenuates norepinephrine-induced cytotoxicity in primary cultured rat cardiac myocytes by antioxidant in vitro. *Journal of Asian Natural Products Research* **11**:5, 417-425. [CrossRef]
20. Fabio Galetta, Giampaolo Bernini, Ferdinando Franzoni, Leonardo Tocchini, Chiara Taurino, Michele Bardini, Marco Rossi, Antonio Salvetti, Gino Santoro. 2008. Preclinical cardiac involvement in phaeochromocytoma: a study with integrated backscatter. *Clinical Endocrinology* **68**:5, 756-761. [CrossRef]
21. Narasimman Gurusamy, Shyamal Goswami, Gautam Malik, Dipak K. Das. 2008. Oxidative injury induces selective rather than global inhibition of proteasomal activity. *Journal of Molecular and Cellular Cardiology* **44**:2, 419-428. [CrossRef]